

Performing effective calculations of protein - ligand binding free energy with the help of molecular dynamics methods

ABSTRACT

Aims: In our study, we aimed to calculate the binding free energies using molecular dynamics methods with the help of biased sampling approach using the binding site residues in protein - ligand complexes and to compare the obtained results with the experimental binding free energies available in the literature.

Methodology: To achieve our goal, we used molecular dynamics and molecular modeling methods such as Steered Molecular Dynamics (SMD) and umbrella sampling. We started our study by selecting the residues in the binding region of the complexes and recording the resulting miniaturized complexes. Then, the structures were reoriented to allow the ligands in the systems we created to be drawn on the z-axis. The ligands in the reoriented structures were pulled on the z-axis using the SMD method and removed from the binding site of the complex, and the poses on the reaction coordinate were recorded. Using the poses selected from the reaction coordinates, 1 ns molecular dynamics simulations were performed for each selected pose using the umbrella sampling method.

Results: As a result of the processes performed, the binding energy was calculated as -7.23 ± 1.75 for the 1NFU complex, -9.73 ± 1.83 for the 2JS4 complex, -9.16 ± 2.53 for the 1FJS complex, -8.63 ± 0.17 for the 1F0R complex and -13.76 ± 2.47 kcal/mol for the 1KSN complex. Experimental values for the mentioned complexes are -10.63 , -10.47 , -10.14 , -10.51 and $+12.90$ kcal/mol, respectively. The differences between the value we obtained as a result of our study and the experimental data vary between 0.8 kcal/mol (1FJS) and 3.4 kcal/mol (1NFU). In addition, there is a correlation of 0.80 between the data we obtained in our study and the experimental results.

Conclusion: The high regression coefficient and low numerical differences between the results we obtained in our study and the experimental results indicate that our approach yields positive results.

Keywords: Umbrella sampling, molecular dynamics, binding energy, factor X_a

1. INTRODUCTION

An important measure of the interaction between proteins and their ligands is the binding free energy. A high binding free energy is an indication that the interaction between protein and ligand is high and the dissociation coefficient of the protein and ligand is low [1]. Accurate calculation of binding free energy is critical for researchers to achieve high success in a short time in designing and obtaining new inhibitor molecules in drug discovery projects [2]. Molecular docking and various molecular dynamics methods are the two most used molecular modeling approaches to estimate binding free energy [3, 4]. Linear interaction energy (LIE) [5], MM/PBSA and MM/GBSA [6], free energy perturbation [7], alchemical approach [8] and biased sampling methodologies [9] are the most common methods used to calculate free energy of binding of protein and ligand complexes.

The most important cause of stroke is atrial fibrillation. The risk of embolism because of atrial fibrillation is high, and the use of anticoagulant drugs in patients with this condition reduces the possible fatal risks [10]. Factor Xa is a critical enzyme that plays a role in the blood clotting process. Therefore, using Factor Xa inhibitors to prevent blood clotting is an approach used to prevent possible embolism. The molecule called warfarin, a vitamin K antagonist, has been the most important oral anticoagulant drug used for decades [11]. Although warfarin is widely used, it has problems such as interactions with many drugs, food, and unexpected pharmacokinetic and pharmacodynamic properties [12]. For this reason, even today, studies continue on the development of novel Factor Xa inhibitors that will have anticoagulant properties [13, 14].

In our study, we aimed to calculate the binding free energies using molecular dynamics methods with the help of a biased sampling approach using the binding site residues in protein-ligand complexes and to compare the obtained results with the experimental binding free energies available in the literature. To carry out these processes, we used some Factor Xa-inhibitor complexes whose binding free energies are known in the literature, which we mention in detail below.

2. MATERIAL AND METHODS

2.1 Hardware and software

All of the simulations were carried out on a workstation equipped with Intel i7 4770K CPU and two NVIDIA Graphics cards GTX 960 and RTX 1050 GPUs running on Ubuntu 18.04 operating system. Atomistic simulations were carried out using Gromacs 2020.6 [15] using Amber99sb [16]. Parameterization of ligands were carried out using AcPype [17] with Anaconda interface [18]. Ligand binding energies were calculated using GromacsWham [19] module. Structure preparations, reorientation and recharging were carried out using PyMol, VMD [20,21] and Chimera [22] software. Graphs were created with the help of Python [23] and Microsoft Office Suite.

2.2 Preparation of the complexes

The structures we use were downloaded from RCSB data bank with the PDB IDs of 1F0R [24], 1FJS [25], 1KSN [26], 1NFU [27], and 2J34 [28]. Each structure was loaded into Pymol one by one and prepared for simulations separately. After loading the structure to Pymol, water molecules were removed. Then, the amino acids of the binding site located within 5 Å of the ligand were identified and copied to be treated as a separate object. If the amino acids around 5 Å of the ligand were selected as a single structure, neighboring amino acids were also included in the structure and chains consisting of at least three amino acids were obtained. In addition, if one or two amino acid gaps occur between the selected chains, the chains are extended by adding the amino acids in between. The chains consisting of the resulting binding site amino acids were renamed and the structure was saved for the process of directing the ligand towards the z-axis. Later, the structure was loaded into the VMD software and its coordinates were updated to orient the ligand to be pulled on the z-axis direction from the binding site. Following this, the dimensions of the resulting structure were determined to establish box dimensions of molecular dynamics simulations. Subsequently, the ligand structure was separated from the complex and loaded into the Chimera software, hydrogens were added to the structure and saved. Following this process, Gromacs compatible parameter files of the ligands were created with AcPype software and used in molecular dynamics simulations. The protein structure obtained in the previous step was used as the starting structure for the molecular dynamics simulations.

2.3 Molecular dynamics simulations

Molecular dynamics simulations were carried out using Amber99sb force field. For steered molecular dynamics (SMD) simulations protein and ligand structures were combined and placed in a rectangular prism water cube whose edges were set to be 1 nm away from the system on x and y axes and four times higher than the dimensions of the complex on z-axis. Complex were centered on x and y axis and set to be 1 nm close to edge on z-axis(Fig 1). Ion concentration of the cube was setted to 0.15 M using Na⁺ and Cl⁻ ions and neutralized.

The energy minimization of the created system was carried out by using the steepest descent minimization method in a maximum of 50000 steps, when the maximum force falls below 10 kJ/mol. The equilibrium process of the energy minimized system was carried out in three steps by using NVT and one steps by using NPTensembles. The positions of the proteins and molecules are fixed using decreasing constrain values (2500, 1000, 500 kJ mol⁻¹ nm⁻² for NVT and 500 kJ mol⁻¹ nm⁻² for NPT simulations) during the equilibrium simulations. NTV equilibrium process was continued for 100 ps with time step 2 fs, the temperature of the system was set to 310 K, V-rescale was used as a thermostat. In NPT equilibrium process, time step 2 fs and simulation time was determined as 100 ps similar to NVT. Brendensen was used as barostat in NPT and 1 bar was used as reference pressure. Short range electrostatic and van der Waals cut-off values were setted to 0.9 nm.

After equilibration ligands was pulled through z-axis with the pulling rate of 0.005 nm/s with the force constant of 1000 kJ mol⁻¹ nm⁻² for 500 ps and coordinates and energy values were recorded for every 10 ps (5000 poses for each run). This process was repeated three times for each ligand. In each run, the time-dependent change in the distance between the ligand and the protein structure was recorded. Selected poses of these replicates were used as starting structures in umbrella sampling (US) simulations.

To calculate the binding energies of the complexes, poses were selected from SMD simulations, taking into account the distances between the protein and ligand structures. For simulations where the distance between protein and ligand was between 0.2 - 1.0 nm, samples were selected every 0.05 nm, and between 1.0 - 2.0 nm, samples were selected every 0.1 nm.

All of the selected poses were equilibrated using Brendensen as barostat in NPT and 1 bar was used as reference pressure before applying US simulations. US simulations were carried out with the pulling rate of 0 nm/s with the force constant of 500 kJ mol⁻¹ nm⁻² to generate poses in the given distance between ligand and protein. At the end of US simulations energy profile of the complex were computed using Gromacs wham module. Binding energies of the complexes were calculated using differences in energies of binded and unbinded complex.

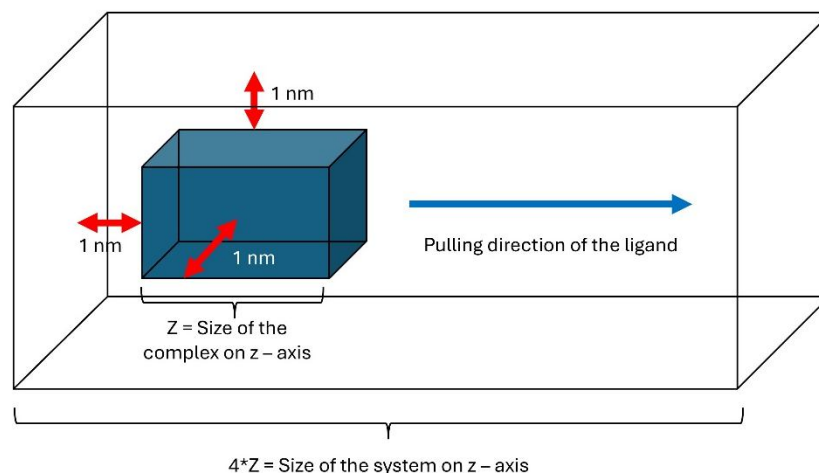


Fig. 1. Dimensions of the systems and pulling direction of the ligands

3. RESULTS AND DISCUSSION

Our aim in our study was to calculate the binding energies in an accelerated manner using simulations using the residue and ligand structures in the binding region of the complex structures we studied. By focusing on the binding pocket of the complexes we studied, we aimed to reduce the volume and number of atoms of the system we worked on and to avoid wasting resources on calculations for residues that do not contribute to binding. Table 1 shows the comparison of the sizes of the systems (binding site and full complex) created for 1F0R, one of the complexes we studied, and the number of atoms they contain. When the Table 1 is examined, it can be seen that volume of the system created using the entire complex is approximately seven times (6.93 times) larger than the system created using binding site residues. When the number of atoms in the systems is compared, it is observed that the entire complex contains approximately seven times (7.3 times) more atoms. We also compared simulation performances of equilibrium and SMD simulation of both systems. For binding pocket system in equilibration phases average simulation rate was 263.80 ns/day and for full complex system this value was 38.28 ns/day. The ratio of simulation rates for equilibration phases is again close to seven with the value of 6.89. Average SMD simulation rates for binding pocket system and full complex system were 168.09 and 26.68 ns/day, respectively. The ratio of simulation rates and SMD phase is close to seven with the value of 6.30, too. These numbers show that, as expected, more calculations can be made per unit time by decreasing the volume of the systems and the number of atoms they contain.

Table 1. Dimensions and sizes of the systems for 1F0R complex

	1F0R	1F0R (Full complex)
Size x (nm)	2.1500	3.7990
Size y (nm)	2.4880	4.5930
Size z (nm)	2.1900	7.3938
Box size x (nm)	4.1510	5.7990

Box size y (nm)	4.4880	6.5930
Box size z (nm)	8.7640	29,575
Volume (nm³)	163,2706	1130.7553
# of total atoms	15753	114791
# of total water molecules	5101	36714

Table 2 contains information about the size and atomic numbers of the systems created by taking into account the binding sites of the complexes we examined in our study. Among these systems, the 1NFU complex has the smallest volume with 125.2538 nm³, while the largest volume belongs to the 1KSN system with 175.7014 nm³. While there are 12527 atoms and 4039 water molecules in the 1NFU system, there are 17166 atoms and 5544 water molecules in the 1KSN system. These numbers are the lowest and highest for 1NFU and 1KSN systems, similar to the volume ranking among the complexes studied.

Table 2. Dimensions and sizes of the systems for binding pocket

	1NFU	2JS4	1FJS	1F0R	1KSN
Size x (nm)	2.0880	2.4390	2.7820	2.1500	2.5430
Size y (nm)	2.2930	2.3580	2.3600	2.4880	2.5760
Size z (nm)	1,8270	1.7980	1.7940	2.1900	2.1190
Box size x (nm)	4.0880	4.4390	4.7820	4.1510	4.5430
Box size y (nm)	4.2930	4.3580	4.3600	4.4880	4.5760
Box size z (nm)	7.3080	7.1920	7.1760	8.7640	8.4760
Volume (nm³)	125.2538	139.1304	149.6162	163,2706	175.7014
# of total atoms	12527	13609	14682	15753	17166
# of total water molecules	4039	4391	4722	5101	5544

Simulation rates of the binding site systems we studied were also examined and summarized in Table 3. As seen in Table 3, it was observed that the simulation speeds decreased as the volumes of the systems and the number of atoms they contain increased, as expected.

Table 3. Simulation rates of binding pocket systems

	1NFU	2JS4	1FJS	1F0R	1KSN
Average simulation rate in equilibrium phase (ns/day)	296.22	269.51	275.88	263.80	251.88
Average simulation rate in SMD phase (ns/day)	241.22	213.59	214.88	168.09	188.74
Average simulation rate in US phase (ns/day)	355.30	331.75	303.61	301.36	274.46

As mentioned in the material method section, US simulations were repeated three times with the help of poses selected from the SMD simulation. The results of three replicates are summarized in Table 4 and show in Figure 2. Simulated binding energy for **1NFU** binding pocket complex is calculated as -7.23 ± 1.75 , for **2JS4** binding pocket complex as -9.73 ± 1.83 , for **1FJS** binding pocket complex as -9.16 ± 2.53 , for **1FOR** binding pocket complex as -8.63 ± 0.17 , for **1KSN** binding pocket complex as -13.76 ± 2.47 kcal/moles. When the results obtained were evaluated, it was observed that the simulations with the highest reproducibility were in the 1FOR binding site system with 0.17 standard deviation value and the lowest in the 1FJS binding site system with 2.53 standard deviation value.

Table 4. Simulated binding energies of binding pocket systems

	1NFU	2JS4	1FJS	1FOR	1KSN
Simulated binding energy for first US simulations (kcal/mol)	-8.06	-11.71	-9.02	-8.71	-16.60
Simulated binding energy for second US simulations (kcal/mol)	-8.41	-9.39	-11.75	-8.43	-12.61
Simulated binding energy for third US simulations (kcal/mol)	-5.22	-8.09	-6.70	-8.74	-12.07
Average simulated binding energy of US simulations (kcal/mol)	-7.23	-9.73	-9.16	-8.63	-13.76
Standard deviations of simulated binding energy of US simulations (kcal/mol)	1.75	1.83	2.53	0.17	2.47

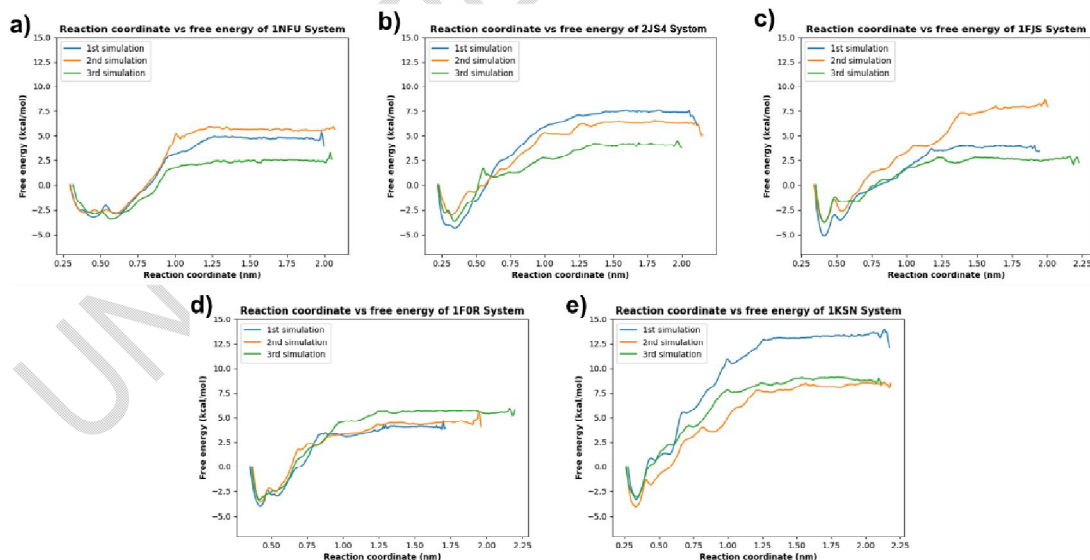


Fig.2. Simulated binding energy graphs of a) 1NFU, b) 2JS4, c) 1FJS, d) 1FOR and e) 1KSN systems

When the results summarized above were compared with the literature information, it was observed that promising values were obtained. Ngo and colleagues worked on four different class of target complexes – cathepsin K (CSTK), type II dehydroquinase (DHQase), heat shock protein 90 (HSP90) and factor Xa (FXa) – on calculation of binding energies using umbrella sampling method [29]. In their paper experimental binding energies for **1NFU** is reported as **-10.63**, for **2JS4** as **-10.74**, for **1FJS** as **-10.14**, for **1F0R** as **-10.51** and for **1KSN** as **-12.90 kcal/mol**. The simulated binding energies obtained in our study, which we summarize in Table 4, and the experimental results are very close to each other. For example, the difference between the simulated binding energy and experimental binding energies in **1KSN** complex was determined as **0.86 kcal/mol**, which are quite close to each other. The largest difference between the simulated binding energy and experimental binding energies was obtained in the **1NFU** complex with a difference of **3.40 kcal/mol**. When the binding energy differences for other complexes were examined, the difference was determined to be **0.98** for **1FJS** complex, **1.01** for **2JS4** and **1.88 kcal/mol** for **1F0R**. For the complexes we examined in our study, information is given about the simulated binding energies using the full complex in the work conducted by Ngo and colleagues. Accordingly, the simulated binding energy for the **1NFU** complex is stated as **-15.43**, **-16.06** for **2JS4**, **-13.48** for **1FJS**, **-12.65** for **1F0R** and finally **-24.45 kcal/mol** for **1KSN**. The differences between the results we obtained in our study and the experimental results are lower than the differences obtained in the study by Ngo and colleagues. In addition, the simulated binding energies calculated in our study are lower than experimental results in all except the **1KSN** complex, while they are higher in all complexes in the study by Ngo and colleagues. All the comparisons mentioned above are summarized in Table 5. Regression analyzes were also performed with the differences in the numbers between simulated binding energies and experimental binding energies. As a result of the analysis, it was determined that there was a regression of **0.80** between the binding energies. To calculate the experimental binding energies of the studied ligands according to the obtained formula, the formula $\Delta G_{\text{EXP}} = 0.400 \Delta G_{\text{US}} - 7.1031$ should be used (Fig 3).

Table 5. Comparison of simulated binding energies obtained in our study and those performed by Ngo and colleagues.

	ΔG_{exp} (kcal/mol)	ΔG_{US^*} (kcal/mol)	$\Delta G_{\text{US}^{**}}$ (kcal/mol)	$\Delta \Delta G_{\text{exp} - *}$ (kcal/mol)	$\Delta \Delta G_{\text{exp} - **}$ (kcal/mol)
1NFU	-10.63	- 7.23	- 15.43	3.40	4.80
2JS4	- 10.74	- 9.73	- 16.06	1.01	5.32
1FJS	- 10.14	- 9.16	- 13.48	0.98	3.34
1F0R	- 10.51	- 8.63	- 12.65	1.88	2.14
1KSN	- 12.90	- 13.76	- 24.45	0.86	11.55

*Results of this study

** Results of Ngo and colleagues

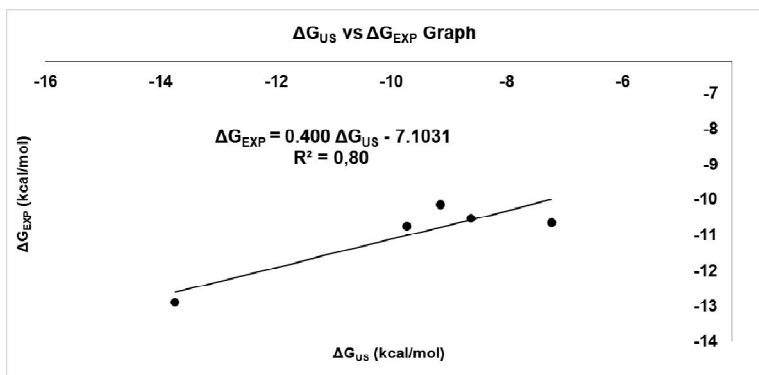


Fig.3.Regression graph of ΔG_{US} vs ΔG_{EXP}

UNDER PEER REVIEW

4. CONCLUSION

Our aim in carrying out this study was to develop a fast and effective approach to calculate the binding energies of protein - ligand complexes. To achieve our goal, it is aimed to bypass the calculations for residues that are not in the binding site in protein-ligand complexes and perform operations for fewer atoms and smaller volumes. With this approach, we observed that during our study, we reduced the working volume and the number of atoms in the system by approximately seven times in the simulations we performed using the residues in the binding site of complex and all residues in the complex. We determined that the simulations we performed with these systems were accelerated approximately 6.5 times. We tried to calculate the protein-ligand binding energies by applying this performance increase on five different factor Xa complexes. As a result of our simulations and calculations, we observed that there were differences of 0.86 to 3.40 kcal/mol between the simulated binding energies and experimental binding energies we obtained. The fact that these values are lower than the values of 2.14 (lowest difference) and 11.55 kcal/mol (highest difference) obtained by Ngo and colleagues [29], who examined the same complexes in the literature, shows that our approach is positive and results comparable to the literature. In addition, the regression between our simulated binding energies and experimental binding energies was also examined. Accordingly, while the regression coefficient we obtained in our study was determined as 0.80, this value was stated as 0.95 in the study conducted by Ngo and colleagues [29]. According to the results obtained in our study, although the differences in terms of binding energies were lower than in the literature, results were lagging the literature in terms of regression. It is very promising and important that with the approach we used in our study, simulation rates of 300 ns/day and higher can be achieved even with outdated hardware resources. It is obvious that simulation rates will increase if current hardware or servers containing GPUs are used, which are available today and whose performance is gradually increasing. In this way, it will be possible to develop and apply molecular dynamics methods or approaches that can obtain results closer to experimental data in a very short time. In our opinion, while our approach enables the binding energy to be calculated with relatively high accuracy in a short time, another contribution it can make to the literature is that it will enable the examination of more than one reaction coordinates, especially in a short time. In this way, more accurate information can be obtained about the binding and dissociation mechanisms of protein and ligand complexes, and binding energies can be calculated with higher accuracy.

CONSENT

It's not applicable.

ETHICAL APPROVAL

It's not applicable.

REFERENCES

1. Borea, P. A., Varani, K., Gessi, S., Gilli, P., & Dalpiaz, A. (1998). Receptor binding thermodynamics as a tool for linking drug efficacy and affinity. *Il Farmaco*, 53(4), 249-254.

2. Cournia, Z., Allen, B., & Sherman, W. (2017). Relative binding free energy calculations in drug discovery: recent advances and practical considerations. *Journal of chemical information and modeling*, 57(12), 2911-2937.
3. Guedes, I. A., de Magalhães, C. S., & Dardenne, L. E. (2014). Receptor–ligand molecular docking. *Biophysical reviews*, 6, 75-87.
4. Deng, Y., & Roux, B. (2009). Computations of standard binding free energies with molecular dynamics simulations. *The Journal of Physical Chemistry B*, 113(8), 2234-2246.
5. de Amorim, H. L. N., Caceres, R. A., & Netz, P. A. (2008). Linear interaction energy (LIE) method in lead discovery and optimization. *Current drug targets*, 9(12), 1100-1105.
6. Hou, T., Wang, J., Li, Y., & Wang, W. (2011). Assessing the performance of the MM/PBSA and MM/GBSA methods. 1. The accuracy of binding free energy calculations based on molecular dynamics simulations. *Journal of chemical information and modeling*, 51(1), 69-82.
7. Wang, J., Deng, Y., & Roux, B. (2006). Absolute binding free energy calculations using molecular dynamics simulations with restraining potentials. *Biophysical journal*, 91(8), 2798-2814.
8. Ngo, S. T., Thai, Q. M., Nguyen, T. H., Tuan, N. N., Pham, T. N. H., Phung, H. T., & Quang, D. T. (2024). Alchemical approach performance in calculating the ligand-binding free energy. *RSC advances*, 14(21), 14875-14885.
9. Kästner, J. (2011). Umbrella sampling. *Wiley Interdisciplinary Reviews: Computational Molecular Science*, 1(6), 932-942.
10. McCarty, D., & Robinson, A. (2016). Factor Xa inhibitors: a novel therapeutic class for the treatment of nonvalvular atrial fibrillation. *Therapeutic advances in cardiovascular disease*, 10(1), 37-49.
11. Yeh, C. H., Fredenburgh, J. C., & Weitz, J. I. (2012). Oral direct factor Xa inhibitors. *Circulation research*, 111(8), 1069-1078.
12. Pinto, D. J., Smallheer, J. M., Cheney, D. L., Knabb, R. M., & Wexler, R. R. (2010). Factor Xa inhibitors: next-generation antithrombotic agents. *Journal of medicinal chemistry*, 53(17), 6243-6274.
13. Zheng, W., Dai, X., Xu, B., Tian, W., & Shi, J. (2023). Discovery and development of Factor Xa inhibitors (2015–2022). *Frontiers in Pharmacology*, 14, 1105880.
14. Zhao, Y., Liu, Q., Du, J., Meng, Q., Sun, L., & Zhang, L. (2024). Accelerating factor Xa inhibitor discovery with a de novo drug design pipeline. *Chinese Journal of Chemical Engineering*.
15. Abraham MJ, Murtola T, Schulz R, Páll S, Smith JC, Hess B, et al. (2015) GROMACS: High performance molecular simulations through multi-level parallelism from laptops to supercomputers. *SoftwareX*, 1, 19- 25.

16. Hornak V, Abel R, Okur A, Strockbine B, Roitberg A, Simmerling C. (2006). Comparison of multiple Amber force fields and development of improved protein backbone parameters. *Proteins*, 65(3), 712-725.
17. Da Silva AWS, Vranken WF. (2012). ACPYPE Antechamber python parser interface. *BMC Res Notes*, 5, 1-8.
18. Anaconda Software Distribution. Computer software. Vers. 2-2.4.0. Anaconda, Nov. 2016. Web. <<https://anaconda.com>>.
19. Hub, J. S., De Groot, B. L., & Van Der Spoel, D. (2010). g_wham A Free Weighted Histogram Analysis Implementation Including Robust Error and Autocorrelation Estimates. *Journal of chemical theory and computation*, 6(12), 3713-3720.
20. Schrödinger, L., & DeLano, W. (2020). PyMOL. Retrieved from <http://www.pymol.org/pymol>
21. Humphrey, W., Dalke, A., & Schulten, K. (1996). VMD: visual molecular dynamics. *Journal of molecular graphics*, 14(1), 33-38.
22. Pettersen, E. F., Goddard, T. D., Huang, C. C., Couch, G. S., Greenblatt, D. M., Meng, E. C., & Ferrin, T. E. (2004). UCSF Chimera—a visualization system for exploratory research and analysis. *Journal of computational chemistry*, 25(13), 1605-1612.
23. Van Rossum, G., & Drake, F. L. (2009). Python 3 Reference Manual. Scotts Valley, CA: CreateSpace.
24. Maignan, S., Guilloteau, J. P., Pouzieux, S., Choi-Sledeski, Y. M., Becker, M. R., Klein, S. I., ... & Mikol, V. (2000). Crystal structures of human factor Xa complexed with potent inhibitors. *Journal of medicinal chemistry*, 43(17), 3226-3232.
25. Adler, M., Davey, D. D., Phillips, G. B., Kim, S. H., Jancarik, J., Rumennik, G., ... & Whitlow, M. (2000). Preparation, characterization, and the crystal structure of the inhibitor ZK-807834 (CI-1031) complexed with factor Xa. *Biochemistry*, 39(41), 12534-12542.
26. Guertin, K. R., Gardner, C. J., Klein, S. I., Zulli, A. L., Czekaj, M., Gong, Y., ... & Pauls, H. W. (2002). Optimization of the β -Aminoester class of factor Xa inhibitors. part 2: Identification of FXV673 as a potent and selective inhibitor with excellent In vivo anticoagulant activity. *Bioorganic & medicinal chemistry letters*, 12(12), 1671-1674.
27. Maignan, S., Guilloteau, J. P., Choi-Sledeski, Y. M., Becker, M. R., Ewing, W. R., Pauls, H. W., ... & Mikol, V. (2003). Molecular structures of human factor Xa complexed with ketopiperazine inhibitors: preference for a neutral group in the S1 pocket. *Journal of medicinal chemistry*, 46(5), 685-690.
28. Senger, S., Convery, M. A., Chan, C., & Watson, N. S. (2006). Arylsulfonamides: a study of the relationship between activity and conformational preferences for a series of factor Xa inhibitors. *Bioorganic & medicinal chemistry letters*, 16(22), 5731-5735.

29. Ngo, S. T., Vu, K. B., Bui, L. M., & Vu, V. V. (2019). Effective estimation of ligand-binding affinity using biased sampling method. *ACS omega*, 4(2), 3887-3893.

UNDER PEER REVIEW